Metamodel-driven optimization of load-adaptive Voronoi lattices for cranial implants using field-based design

Alexander Seidler[1,*], Philipp Sembdner[1], Kristin Paetzold-Byhain[1]

[1] Chair of Virtual Product Development, Dresden University of Technology (TUD)

** Corresponding author:*
Alexander Seidler
George-Bähr-Straße 3c
01062
Dresden
☎ *+49 351/463-39138*
✉ *alexander.seidler@tu-dresden.de*

Abstract

This study presents a metamodel-driven optimization of load-adaptive Voronoi lattices for cranial implants using field-based control of geometric parameters. A metamodel was established by varying cell size in loaded and beam diameter in unloaded regions, enabling stiffness predictions with 1.2 % accuracy and a coefficient of prognosis of 0.86. Sensitivity analyses showed a strong influence of beam diameter (r = 0.94) and a moderate effect of cell size (r = –0.46) on the lattice stiffness. The optimized lattice achieved bone-like stiffness with a safety factor of 2.5 under physiological loads, demonstrating the efficacy of Voronoi-based, field-controlled design as design element in implants.

Keywords

Voronoi, implicit modelling, lattice, optimization, cranial implants

 | DOI: 10.35199/dfx2025.12

1. Introduction

The integration of individualized therapy with bone replacement implants remains a substantial challenge in the design process. In the case of permanent implants, the emphasis is on precise adaptation to the stresses of the surrounding bone tissue to prevent bone loss induced by stress shielding. In this regard, alternative materials such as polyetheretherketon (PEEK), polymethylmethacrylat (PMMA), and calcium phosphate cements (CPC) have been utilized as alternatives to the bioinert materials CoCrMo and Ti6Al4V [1–4]. Lattice structures have also seen increased utilization in reducing stiffness gradients between implants and bone tissue or in serving as a matrix for facilitating bone ingrowth [3]. This enhancement of biomechanical integration has been demonstrated to be a key factor in reducing stress shielding.

CPC implants with lattice structures are the subject of intensive research for the treatment of bone defects in the skull region [2, 5]. These implants are designed to support bone healing by specifically promoting the body's own bone formation during the decomposition of the material. As such, they represent one of the few forms of therapy for the body's own healing of large-area skull defects. However, due to its brittle material properties, CPC is susceptible to implant failure even under low loads. In response to these findings, Pendzik et al. [5] developed a hybrid implant concept that combines a supporting structure with a carrier made of PEEK or PMMA. This combination was designed to improve the load-bearing capacity and implantability of cranial CPC implants. However, these implants remain vulnerable to external stresses, necessitating the implementation of supplementary protective measures, such as helmet use, until the complete resolution of the CPC. Furthermore, the inadequate load-bearing capacity of CPC diminishes the acceptance of such implants in cranial skull care. A potential strategy to enhance this acceptance is the implementation of temporary protective implants, which ensure the safety and stability of the implant until complete resorption of the CPC.In this context, lattice structures designed specifically according to the principles of load adaptation are becoming increasingly important [3, 6–8]. Koch [9] proposes a categorization of lattice structures into three types: regular, pseudoperiodic, and irregular. The irregular type is particularly advantageous due to its flexibility in design and adaptation to different requirements. Irregular lattice structures, particularly those derived from Voronoi diagrams, hold considerable promise due to their foundation on the distribution of seed points within the design space. This characteristic facilitates precise modulation of stiffness [4, 6–8]. The topology of Voronoi structures can be defined by the number and arrangement of seed points, with the cell shape being described by a cell metric that includes its size, aspect ratio, orientation, and the number and length of edges and pore sizes [9].The utilization of scalar field functions facilitates the arrangement of these cells, thereby establishing a heterogeneous structure and modulating the stiffness within the implant in accordance with the inherent characteristics of the natural bone structure [7]. This adjustment facilitates the emulation of the stiffness of the bone to be replaced, thereby minimizing bone remodeling initiated by stress shielding [3].

This investigation explores the design of Voronoi lattices to ensure the desired stiffness of the replacement bone while maintaining minimal component height, thereby facilitating an implant design that conforms to the contours of the skull. The goal of this research is to engineer an implant that provides a protective barrier for cranial CPC implants, shielding them from external forces until complete resorption has occurred. The finite element analysis (FEA) is employed to analyze the stiffness of different Voronoi structures using Ansys Mechanical. This analysis is used to develop an approach for controlling the design parameters that ensures bone-like stiffness of the lattice structure. For this purpose, a metamodel based on numerical investigations is being developed. This metamodel will significantly reduce development time in the future and enable the successful overcoming of the difficulties in development.

2. Material & Methods

2.1. Data preparation

For the present study, anonymized data sets from the AutoImplant Challenge [10, 11] were utilized. The data set employed (sub11) is available in Nearly Raw Raster Data (NRRD) format and has a layer spacing of 1.2325 mm and a pixel spacing of 0.4883 mm. The extraction of the skull bone and the implant body that closed the defect was achieved by selecting an appropriate threshold value and creating isosurfaces using the Marching Cubes algorithm. These surfaces were then saved in STL format. This was imported into the nTop software and converted into a voxel grid with a grain size of 0.1 mm. Subsequently, the grid was subjected to a linear smoothing algorithm, employing a grain size of 1 mm. The mean distance to the original data was 0.28 mm, indicating that, despite the smoothing, a low deviation from the original data was maintained. Furthermore, all patient data was aligned according to the fracture, thereby defining reproducible, patient-specific coordinate systems in the area of the bone defect. The origin of this coordinate system is defined by the center of mass of the implant body closing the bone defect, which is projected onto the outer surface. The Z-axis is defined by the surface normal at this particular point, while the X-axis is defined by the direction vector of the furthest point of the defect. This coordinate system functions as a global reference system in the investigation. As the available data did not include information regarding the thickness of the cortical bone in isolation, this was defined by a field function based on the investigative results of Lillie et al. [12]. The thickness of the cortex decreases from the face to the back of the head. Therefore, the model is developed using a distance field along the Y-axis of the global coordinate system. The thickness of the cortex in the parietal region of the skull is defined as between 1 mm and 1.13 mm according to the results of Lillie et al. [12].

2.2. Geometry synthesis of load adaptive Voronoi lattice

The employment of Voronoi diagrams in the design of load-adaptive lattice structures has been demonstrated to exhibit considerable promise, as substantiated by Koch [9]. The Voronoi structure can be subdivided into two-dimensional and three-dimensional structures. In this study, form-following two-dimensional (2D) Voronoi diagrams are employed to generate lattice structures with a circular cross-section. The software *nTop* is used to create three-dimensional models. The structure is characterized by the distribution of points along the external surface of the bone fragment. Consequently, the points are distributed randomly on the surface using a random seed. In this study, a random distribution of points was employed, with random seeds 1 and 30 relaxation iterations for the most uniform distribution of seed points in nTop.

A control field is defined to achieve heterogeneous cell sizes and beam diameters. The configuration of this control field is predicated on the total deformation of the bone fragment intended for replacement. For this purpose, the simulation data from Ansys Mechanical is imported into nTop as a point cloud and converted into a scalar field (Fig. 1, left). Subsequently, the deformations are normalized to define the control field within the scale range of 0 to 1 (Fig. 1, middle left). The cell size (**CS**) (Fig. 1, middle right) is subsequently described based on the control field utilizing a scalar field, wherein $\mathbf{CS_{min}}$ signifies the minimum seed point spacing and, consequently, the minimum cell size, and $\mathbf{CS_{max}}$ delineates the maximum cell size. These values are mapped onto the control field, and all values in between are determined by linear interpolation. This delineates a continuous scalar field of the cell size. The same procedure is used for the beam diameter (**d**) (Fig. 1 right). In regions exhibiting high levels of stress (control field = 1), cells are defined by a maximum seed point spacing ($\mathbf{CS_{max}}$) of 10 mm or less and a maximum beam diameter ($\mathbf{d_{max}}$) of 10 mm or less. In the unloaded areas (control field = 0), a $\mathbf{CS_{min}} \geq 1.5$ mm and $\mathbf{d_{min}} \geq 0.5$ mm are defined. It is evident that this also serves as a preventative measure against cell closure, a phenomenon that can arise due to unfavorable combinations of beam diameter and cell size.

Furthermore, a maximum seed point quantity of 500 is delineated to ensure sufficient flexibility in reacting to load cases, as smaller seed point quantities yield a reduced number of cells, thereby diminishing the structural response to load cases. The adaptive structure is thus described by four global structure parameters: the minimum and maximum beam diameter and the minimum and maximum seed point spacing, which describe the cell size.

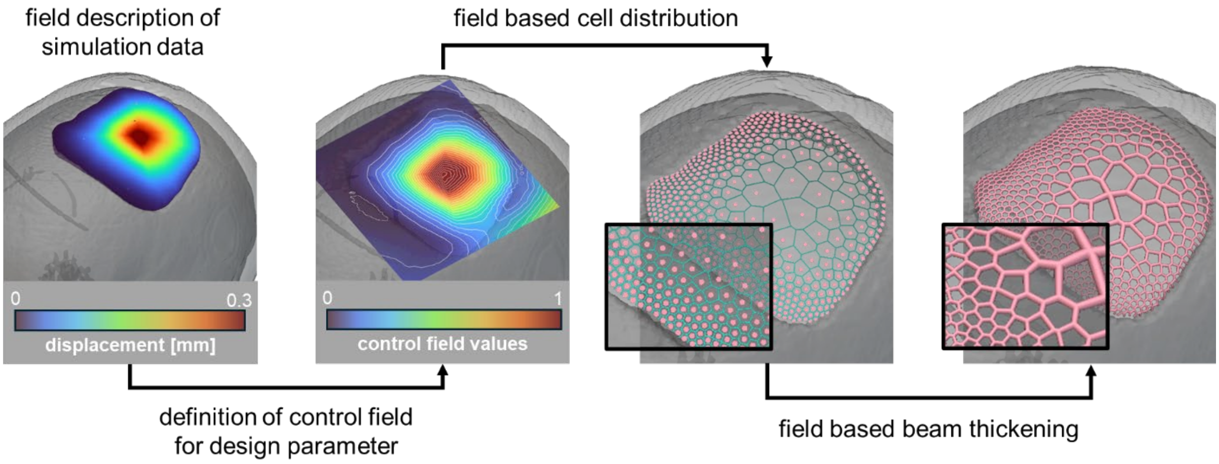

Fig. 1: Design approach for load-adaptive design of Voronoi lattices for cranial implants

The values enumerated for the parameters of the adaptive Voronoi structure signify the maximum and minimum values of the respective parameters. The objective of the present study is to replace the bone stiffness of the missing bone area. Therefore, full factorial parameter studies are carried out for these structural parameters. It is first considered that $\mathbf{d_{max}}$ = 2 mm and $\mathbf{CS_{min}}$ = 1.5 mm are defined as constants. Next, it is considered that $\mathbf{CS_{max}}$ = [5.0, 7.5, 10.0] mm and $\mathbf{d_{min}}$ = [0.5, 0.75, 1.0] mm are varied as discrete variables with interval scale levels. This parameter definition ensures that the structures can be manufactured. A total of nine design samples are derived (Tab. 1), which correspond to adaptively adjusted lattice structures, taking these different parameter values into account. Moreover, the mass ($\mathbf{m_{Lattice}}$) and porosity were determined based on geometry models. Subsequently, these specimens are examined under identical load conditions to determine the structural stiffness.

Tab. 1: Design sampling of different load-adapted Voronoi structures

ID	1	2	3	4	5	6	7	8	9
$\mathbf{d_{min}}$ [mm]	0.50	0.75	1.00	0.50	0.75	1.00	0.50	0.75	1.00
$\mathbf{CS_{max}}$ [mm]	5.00	5.00	5.00	7.50	7.50	7.50	10.0	10.0	10.0
$\mathbf{m_{Lattice}}$ [g]	6.05	8.41	11.1	5.53	7.83	10.5	5.10	7.38	10.0
Porosity [%]	61.3	54.9	48.6	64.8	58.0	51.2	67.3	60.4	53.7

In addition to the lattice structures, a solid contour is defined as the edge structure for the implant, which acts as a protective component, enabling continuous contact with the skull bone. The configuration of the edge structure is determined by the specific fracture characteristics of each individual fracture. The application of various discretization steps, including CT imaging and surface modeling, results in the formation of a discrepancy between the bone fragment (Fig. 2, left, yellow) and the skull bone (Fig. 2, left, gray). Consequently, a distance field (Fig. 2, left) is generated based on this gap and constrained by two thresholds: 0 mm (bone fragment) and 4 mm (skull bone). This distance field is employed to thicken the bone fragment, thereby closing the gap with an accurate contour (Fig. 2, middle, yellow). Subsequent to this, employing Boolean operations, the volume of the bone fragment and the skull bone is subtracted from the resulting geometry. The resulting geometry (Fig. 2, right, blue) is then smoothed and combined with the volume of the lattice structure (Fig. 2, right, red) using Boolean union.

In this investigation, the contour width was simplified to generate the edge contour. In order to compare the stiffness between the bone fragment and the implant, the contour width in this investigation was set equal to the bone thickness. This ensured that the contact conditions in the stiffness investigations were equivalent. However, this simplification does not impact the stiffness investigations of the lattice structures, as the stiffness determination evaluates the resistance of the stamp displacement to the lattice structure. The edge area does not interfere with the lattice structure in this regard. To facilitate a comprehensive analysis of the bone's overall structure and its deformation behavior, it is imperative to modify the edge structure through additional refinements.

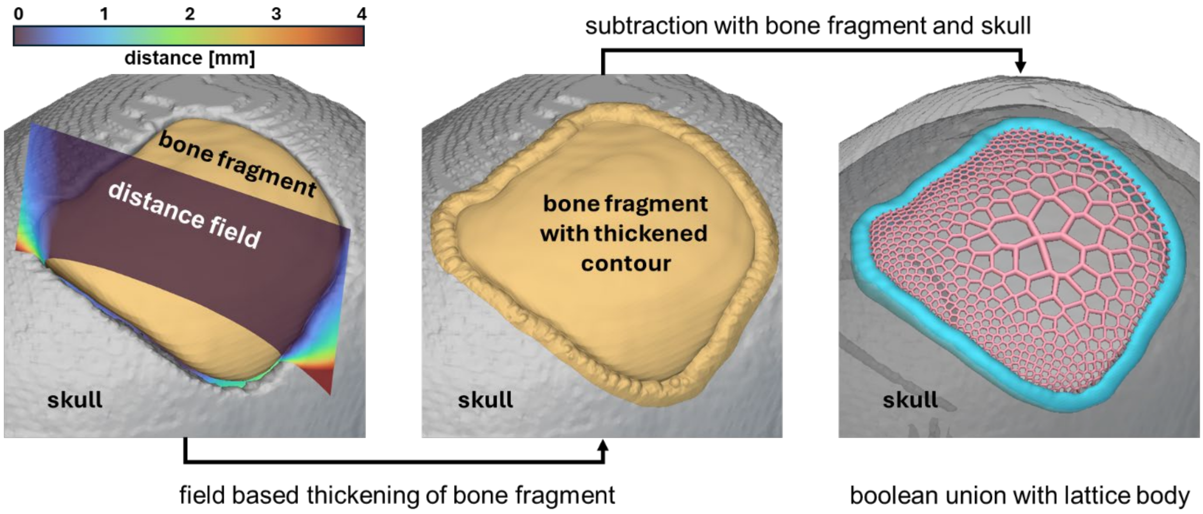

Fig. 2: Synthesis of conture geometry and design of load-adpated cranial implant

2.3. Simulation model

In the current state, there are no standard load scenarios for designing and testing the load-bearing capacity of skull bone replacement implants. This is due to the fact that different scenarios may be relevant depending on the area of the skull to be replaced and the loads that occur in everyday life and during sporting activities. Therefore, a static pressure load that can be reproduced experimentally was selected as the scenario and implemented in *Ansys Mechanical (version 2024 R2)* (Fig. 3).

The implant and the bone fragment to be replaced are loaded at the center of mass and projected onto the surface by a stamp with a quasi-static displacement ($\mathbf{s}_{\mathbf{Stemp}}$) of max. 0.3 mm. The stamp features a spherical tip with a radius of 12.5 mm. The implant is situated on a fixed base plate. It is assumed that both the stamp and the base plate are rigid bodies. For the purpose of modeling the contacts between the inspected object and the stamp (Fig. 3, green) and between the inspected object and the base plate (Fig. 3, yellow), frictionless contact is assumed. The contact surfaces are additionally adjusted to touch in order to mitigate the influence of the contact reaction forces on the measurements. The reaction forces occurring in the stamp are calculated for a total displacement of 0.3 mm for the bone fragment (Fig. 3, circle) and the lattice design variants (Tab. 1). The structural stiffness is then derived from the ratio of the displacement and the reaction force.

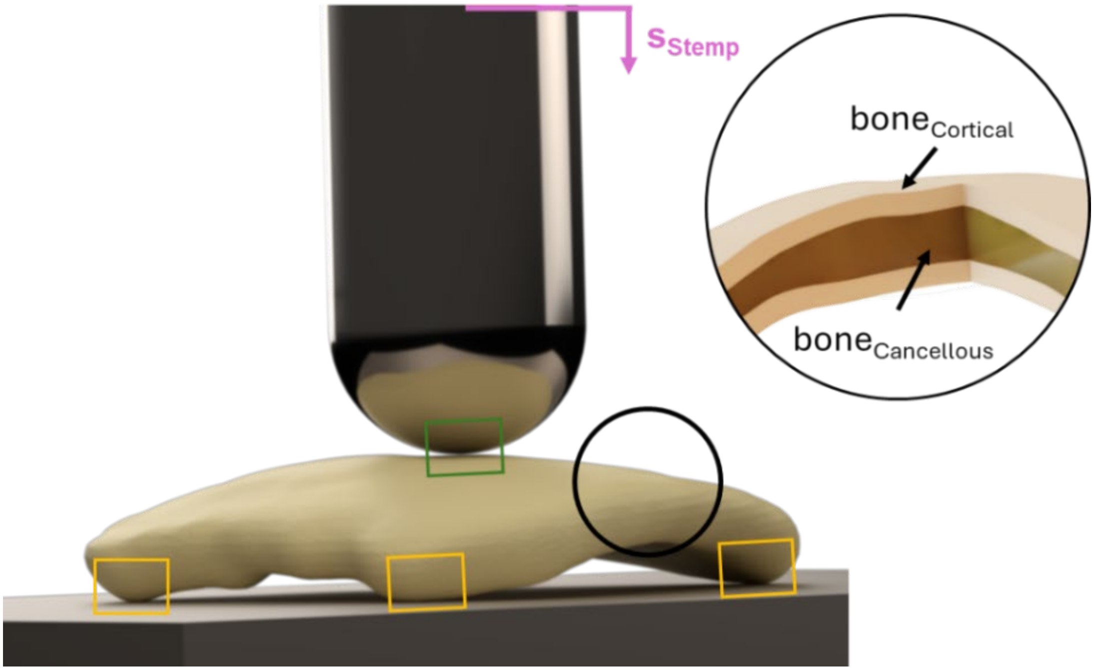

Fig. 3: Simulation model for structural stiffness investigation

The titanium alloy (Ti6Al4V) is specified for the implants, which is realized by an elastoplastic material model with a bilinear isotropic hardening model (Tab. 2). This model is employed to map elastoplastic deformation states during investigations of the various lattice structures (Tab. 1). For the material models of the bone (Fig. 3, circle), the results of the investigations by Schröter et al. [13] for the cortical bone and Wagoner et al. [14] for the cancellous bone were used (Tab. 2).

Tab. 2: Material models for FEA

Material	Density [kg/m³]	Young's modulus [GPa]	Poisson's ratio **v**	Tensile yield strength [MPa]	Tangent modulus [GPa]
Cortical Bone	1900	16	0.46	100	
Cancellous Bone	150	0.3	0.3	3	
Ti6Al4V	4405	107	0.323	1098	1332

Mesh independence study

In order to estimate numerical inaccuracies in the simulation model caused by discretization errors, a mesh independence study is performed on a simplified lattice structure with 100 seed points and a bar diameter of 0.5 mm. The representation of thin bars in the mesh is the greatest challenge in the meshing of lattice structures. Tetrahedrons with a quadratic approximation function were utilized for meshing. The element sizes of the meshes were 1 mm (M1), 0.5 mm (M2), and 0.25 mm (M3). Subsequently, employing a mesh with an element size of 0.5 mm, the deviation of the determined reaction forces and the equivalent maximum stresses that occurred were determined. The maximum reaction force between M1 and M2 exhibited a deviation of 0.43 %, while the stresses demonstrated a deviation of 7 %. Conversely, the discrepancy between M2 and M3 diminished considerably, with the reaction force exhibiting a deviation of 0.17 % and the stress a deviation of 0.26 %. This signifies that the simulations are executed employing the M2 element size.

3. Results

For all design variants (Tab. 1), the reaction force was determined via the stamp displacement (Fig. 4). Furthermore, the curve of the bone fragment to be replaced was plotted as the target curve, with a maximal force of 153.87 N at 0.3 mm stamp displacement (Fig. 4, blue). Design 3 (Fig. 4, yellow) demonstrated the highest degree of resistance to deformation with 240.3 N, while Design 4 exhibited the lowest degree of resistance to deformation with 133.0 N (Fig. 4, green). It is evident that the curves of design 1 (Fig. 4, light blue) and design 3 (Fig. 4, yellow) deviate from the other curves. This is due to a change in the contact status of these designs, specifically in one contact between the base plate and the implant. However, this lifting off of the implant has no effect on the maximum structural lattice stiffness.

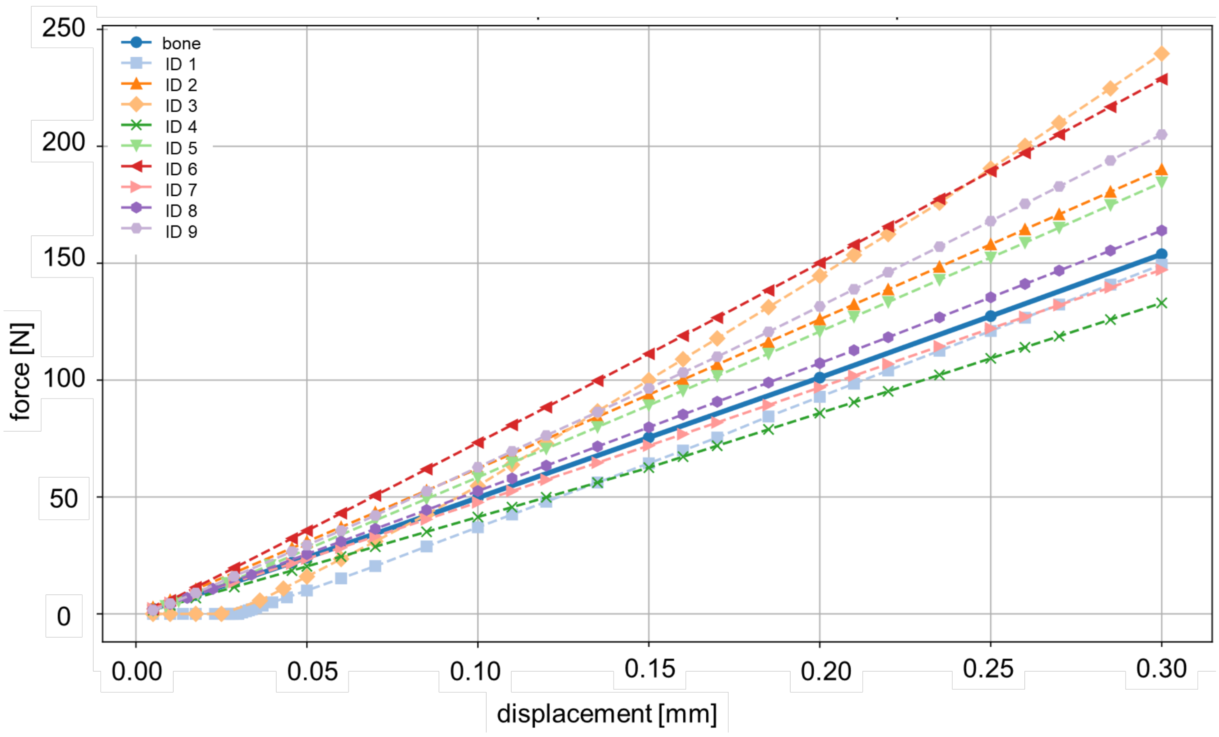

Fig. 4: Force-displacement curve of every design variation and the bone fragment

In light of these findings, the maximum stiffness of the structures under this load was also examined. Subsequently, a response surface was created using second-order polynomial approaches, and the corresponding mass of the design variants was plotted on the response surface using a mapped color map (Fig. 5). Additionally, the isoline for bone stiffness, which was determined to be 512.86 N·mm^{-1}, was represented by a black line. Therefore, it is evident that the metamodel can be utilized to investigate the optimal design parameters for the adaptive design of Voronoi structures along the isoline. The objective is to map bone-like stiffness with the lattice structure by minimal mass of implant. The optimal design is characterized by a minimum beam diameter of 0.62 mm and a maximum cell size of 9.65 mm (Fig. 5, yellow circle) and has a predicted minimum mass of 6.23 g, which lies within the bootstrapped 95% confidence interval of [5.17, 6.66] g (mean: 5.87 g), indicating reasonable consistency between model prediction and resampled estimates. The predicted porosity of the lattice structure is 63.5 %.

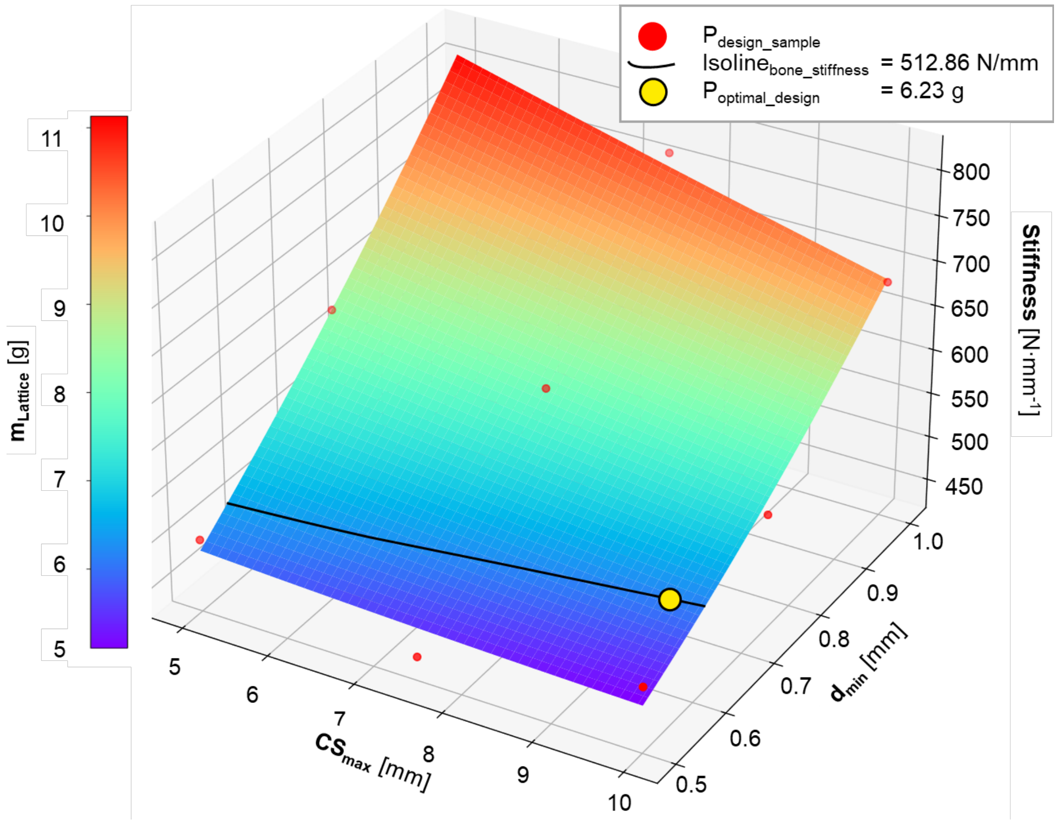

Fig. 5: Metamodel of design parameter for load-adaptive Voronoi structure replicating bone stiffness

Consequently, the mass-optimized design was evaluated under identical conditions, resulting in a calculated stiffness of 506.3 $N{\cdot}mm^{-1}$. The maximum equivalent stress (**σ_V**) of the implant structure is 431 MPa (Fig. 6a), which corresponds to a safety factor (**FoS**) of 2.5 (Fig. 6b). When subjected to an identical load, the bone fragment demonstrated a comparative stress of 150 MPa, which corresponds to a safety factor of 1. Moreover, the implant was inserted into the skull bone model to verify the fit in accordance with the aesthetic boundary conditions (Fig. 6c).

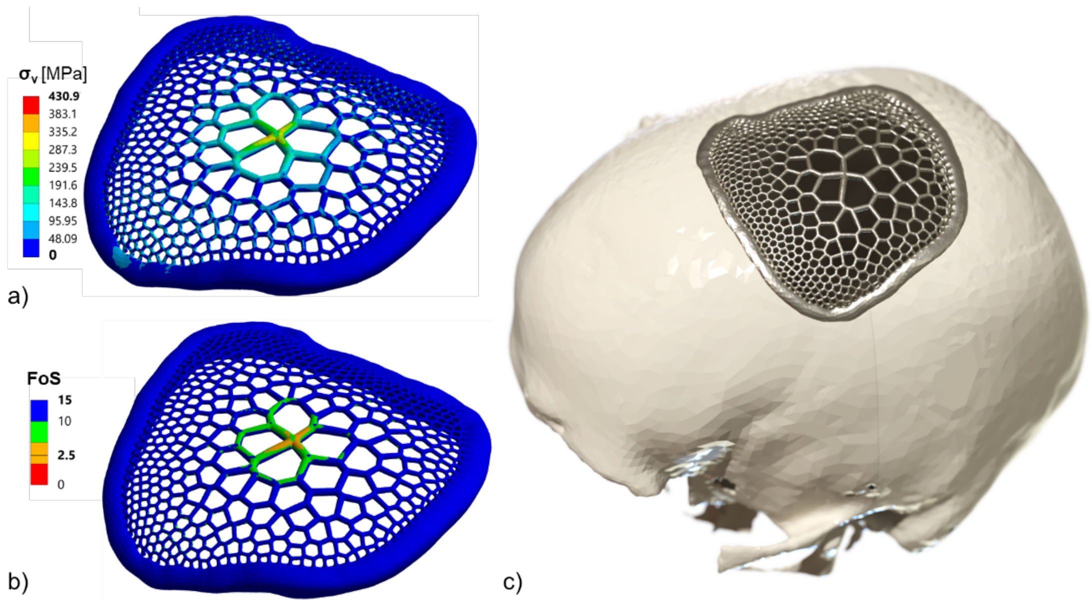

Fig. 6: a) Equivalent stress of the optimized cranial implant; b) factor of safety for Ti6Al4V; c) fit verification of the optimized cranial implant

4. Discussion

The findings of this study demonstrate that the stiffness of Voronoi lattice structures can be accurately and load-adaptively adjusted through the implementation of implicit methods and field-based control of the geometric parameters. The investigations confirm that a differentiated design is necessary to achieve minimum component masses and high porosities with a given structural stiffness. In areas with significant loading and substantial deformations, the utilization of large cells with thick beams is recommended. Conversely, in areas with minimal loading, the employment of small cells with thin beams is advantageous. The developed metamodel, based on minimal sampling quantities, enables the required design parameters for a target stiffness to be predicted with an accuracy of 1.28 % and a coefficient of prognosis of 0.86. Consequently, it offers an effective foundation for the design of load-adapted lattice structures.

The sensitivity analyses demonstrate that $\mathbf{CS_{max}}$ has a moderate effect on structural stiffness (r = -0.46). Consequently, a decrease in cell size in loaded areas results in a modest increase in stiffness. Conversely, $\mathbf{d_{min}}$ exhibited a robust linear correlation with stiffness (r = 0.94), underscoring the preeminent impact of this parameter on the mechanical properties. Additionally, the findings suggest analogous patterns in the impact of the parameters on mass and porosity. Given the direct proportionality between mass and stiffness, as well as the indirect proportionality between porosity and mass, it can be concluded that the observed sensitivities are largely reflected in these target variables. However, in the context of structural porosity, there is a marginal deviation from this norm, as evidenced by the slightly different parameters $\mathbf{CS_{max}}$ (r = 0.54) and $\mathbf{d_{min}}$ (r = -0.94). Consequently, minimizing the mass invariably results in maximizing the porosity. These sensitivities are reflected in the selection of the optimal design parameters. The objective was to achieve a bone-like stiffness with minimum mass. To this end, $\mathbf{CS_{max}}$ was reduced by 3.5 % of the maximum cell size, and $\mathbf{d_{min}}$ was increased by 24 % of the minimum possible diameter.

The resulting Voronoi structure exhibited a stiffness of 506.3 $N \cdot mm^{-1}$, which is comparable to that of the bone fragment, with a deviation of only 1.28 %. This deviation is primarily attributable to the limited number of data points available for the metamodel, a deficiency that can be resolved in the future through the incorporation of additional data. The failure limit of the bone was also considered in this study. The optimized lattice structure achieves a factor of safety of up to 2.5 under the same load, and therefore, it can withstand loads of up to 375 N without plastic deformation. Consequently, the implant is within the load range specified by Khan [15]. The high porosity of the Ti alloy lattice also reduces artifacts in CT images [16], which is particularly important for skull defects with CPC implants in order to better monitor bone regeneration. The results demonstrate the efficacy of Voronoi diagrams in generating load-adaptive lattice structures, facilitating the realization of implants with bone-like stiffness, even in limited implantation spaces.

5. Conclusion

This work systematically investigated the suitability of Voronoi structures as structural elements for protective components of cranial hybrid implants and their load-adaptive design. A metamodel was developed that enables the design of load-adaptive Voronoi lattices with a prediction accuracy of 1.2 %. This metamodel was developed by varying the parameters of maximum cell size in loaded areas and minimum beam diameter in unloaded areas. This enables the precise calibration of stiffness, contingent upon other target variables, including mass and porosity. The selected parameters yielded a mass-optimized Voronoi lattice with bone-like stiffness, capable of withstanding significantly higher loads than the replaced bone fragment due to a safety factor of 2.5. This finding underscores the efficacy of Voronoi-based load-adaptive design in the efficient dimensional estimation of protective implants.

Beyond the geometric parameters investigated, the Voronoi diagram offers additional design parameters that should be integrated into the metamodel in future work to further improve adaptation to specific load scenarios. Furthermore, material substitutions, such as PEEK or PMMA, should be investigated to realize alternative protective implants with reduced allergy risk and new manufacturing possibilities.

Acknowledgement

This work was supported by the European Union (EFRE) and by the Saxon State Parliament within the framework of the project "AdInKranio" (grant number: 100741563).

References

[1] Bonda, David J. ; Manjila, Sunil ; Selman, Warren R. ; Dean, David: *The Recent Revolution in the Design and Manufacture of Cranial Implants: Modern Advancements and Future Directions*. In: *Neurosurgery* 77 (2015), Nr. 5, 814-24; discussion 824

[2] Holtzhausen, Stefan ; Sembdner, Philipp ; Pendzik, Martin ; Schmidt, Holger Wilhelm Rudolf ; Paetzold-Byhain, Kristin: *Additive manufacturing of individual bone implants made of bioresorbable calcium phosphate cement using the example of large skull defects*. In: *Proceedings of the Design Society* 4 (2024), S. 1757–1768

[3] Chao, Long ; He, Yangdong ; Gu, Jiasen ; Xie, Deqiao ; Yang, Youwen ; Shen, Lida ; Wu, Guofeng ; Wang, Lin ; Tian, Zongjun ; Liang, Huixin: *Design of porous structure based on the Voronoi diagram and stress line for better stress shielding relief and permeability*. In: *Journal of Materials Research and Technology* 25 (2023), S. 1719–1734

[4] Sharma, Neha ; Ostas, Daniel ; Rotar, Horatiu ; Brantner, Philipp ; Thieringer, Florian Markus: *Design and Additive Manufacturing of a Biomimetic Customized Cranial Implant Based on Voronoi Diagram*. In: *Frontiers in physiology* 12 (2021), S. 647923

[5] Pendzik, Martin ; Holtzhausen, Stefan ; Heinemann, Sascha ; Paetzold, Kristin: *Further development f the design process for hybrid individual implants*. In: *Proceedings of the Design Society* 3 (2023), S. 2035–2044

[6] D'Andrea, Luca ; Goretti, Giorgio ; Magrini, Gianni ; Vena, Pasquale: *Tuning the trabecular orientation of Voronoi-based scaffold to optimize the micro-environment for bone healing*. In: *Biomechanics and modeling in mechanobiology* 24 (2025), Nr. 3, S. 1057–1071

[7] Cao, Wei ; Pan, Wenjun ; Liu, Bin ; Lu, Ping ; Lin, Hanxuan ; Huang, Jinwang: *Gradient anisotropic design of Voronoi porous structures*. In: *International Journal of Mechanical Sciences* 278 (2024), S. 109484

[8] Liu, Bin ; Li, Shangting ; Cao, Wei ; Lu, Weihong ; Lu, Ping: *Design of 3D anisotropic Voronoi porous structure driven by stress field*. In: *Computer Methods in Applied Mechanics and Engineering* 420 (2024), S. 116717

[9] Koch, Peter: *Funktionale Voronoi-Gitterstrukturen für die Additive Fertigung*. Dresden : Technische Universität Dresden, 2024

[10] Ellis, David G. ; Aizenberg, Michele R.: *AutoImplant 2021 Task 2 - Clinical Cases Requiring Cranioplasty*. 2021

[11] Li, Jianning ; Ellis, David G. ; Pepe, Antonio ; Gsaxner, Christina ; Aizenberg, Michele R. ; Kleesiek, Jens ; Egger, Jan: *Back to the Roots: Reconstructing Large and Complex Cranial Defects using an Image-based Statistical Shape Model*. In: *Journal of medical systems* 48 (2024), Nr. 1, S. 55

[12] Lillie, Elizabeth M. ; Urban, Jillian E. ; Weaver, Ashley A. ; Powers, Alexander K. ; Stitzel, Joel D.: *Estimation of skull table thickness with clinical CT and validation with microCT*. In: *Journal of anatomy* 226 (2015), Nr. 1, S. 73–80

[13] Schröter, Lena ; Kaiser, Friederike ; Stein, Svenja ; Gbureck, Uwe ; Ignatius, Anita: *Biological and mechanical performance and degradation characteristics of calcium phosphate cements in large animals and humans*. In: *Acta biomaterialia* 117 (2020), S. 1–20

[14] Wagoner Johnson, Amy J. ; Herschler, Brad A.: *A review of the mechanical behavior of CaP and CaP/polymer composites for applications in bone replacement and repair*. In: *Acta biomaterialia* 7 (2011), Nr. 1, S. 16–30

[15] Khan, Mohammad Zahid ; Bhaskar, Jitendra ; Kumar, Anand: *Design and analysis of strut-based lattice structure cranial implant*. In: *Journal of Mechanical Engineering and Sciences* (2023), S. 9307–9314

[16] Carter, Luke N. ; Addison, Owen ; Naji, Nashwan ; Seres, Peter ; Wilman, Alan H. ; Shepherd, Duncan E. T. ; Grover, Liam ; Cox, Sophie: *Reducing MRI susceptibility artefacts in implants using additively manufactured porous Ti-6Al-4V structures*. In: *Acta biomaterialia* 107 (2020), S. 338–348